ANNUAL SUMMARIES

Atlantic Hurricane Season of 1992

MAX MAYFIELD, LIXION AVILA, AND EDWARD N. RAPPAPORT

National Hurricane Center, NWS, NOAA, Coral Gables, Florida

ABSTRACT

The 1992 hurricane season is summarized, including accounts of individual storms. Six tropical storms were tracked, of which four became hurricanes. In addition, one subtropical storm formed during the year. The season will be remembered most, however, for Hurricane Andrew. Although Andrew was the only hurricane to make landfall in the contiguous United States during 1992, it earned the distinction of becoming the most expensive natural disaster in United States history.

1. Introduction

The National Hurricane Center (NHC) identified and tracked six tropical storms and one subtropical storm in the Atlantic–Gulf of Mexico–Caribbean region during 1992. Of the six tropical storms, four developed into hurricanes. These totals are less than the past 50-yr average of 9.8 tropical storms and 5.7 hurricanes. In addition, three other tropical cyclones developed. They were tropical depressions that did not reach tropical storm status.

Subtropical storm, tropical storm, and hurricane tracks from 1992 are shown in Fig. 1. The tracks show that no system reached hurricane intensity south of 25°N. This is the second year in a row that this occurred. Additional season statistics are given in Table 1.

According to Neumann et al. (1990), April is the only month during which no tropical or subtropical cyclone with a 1-min wind speed greater than or equal to 17 m s^{-1} has formed. The appearance of the subtropical storm in April of 1992, then, has some significance for keepers of such records. However, subtropical cyclones have been tracked only since 1968 (tropical cyclone records go back to 1871) and it is possible that some systems that were designated extratropical prior to 1968 could have been subtropical.

Although a below-average number of tropical storms occurred, 1992 will be remembered for producing Hurricane Andrew, the year's only major hurricane (wind speeds greater than or equal to 50

m s^{-1}) and the most expensive natural disaster in United States history. Andrew was a small and ferocious "Cape Verde" system that wrought unprecedented economic devastation along a path through the northwestern Bahamas, the southern Florida peninsula, and south-central Louisiana. Damage in the United States is estimated at \$20–\$25 billion. The tropical cyclone struck southern Dade County, Florida, especially hard, with violent winds and storm surges characteristic of a category 4 hurricane on the Saffir–Simpson hurricane scale (Simpson 1974) and with a central pressure (922 mb) that is the third lowest this century for a hurricane at landfall in the United States. In Dade County alone, the forces of Andrew resulted in 15 deaths and up to one-quarter million people homeless. The direct loss of life seems remarkably low considering the destruction caused by this hurricane.

It is interesting to note in Fig. 2 the area of weaker than normal vertical shear of the horizontal wind over the tropical Atlantic during the month of August. This pattern is representative of the conditions that were observed in Andrew's environment during the cyclone's rapid intensification phase. However, there was a significant increase of vertical shear over much of the tropical Atlantic during September (Fig. 3). This was mainly related to an increase of upper-tropospheric westerlies to the east of the Lesser Antilles during the climatological peak period of tropical cyclone frequency. In September, the general region of formation shifted toward higher latitudes, to where lighter shear prevailed, and disturbances of nontropical origin led to the development of tropical cyclones (Pasch and Avila 1994).

Corresponding author address: Max Mayfield, NHC/NWS/NOAA, 1320 South Dixie Highway, Coral Gables, FL 33146.
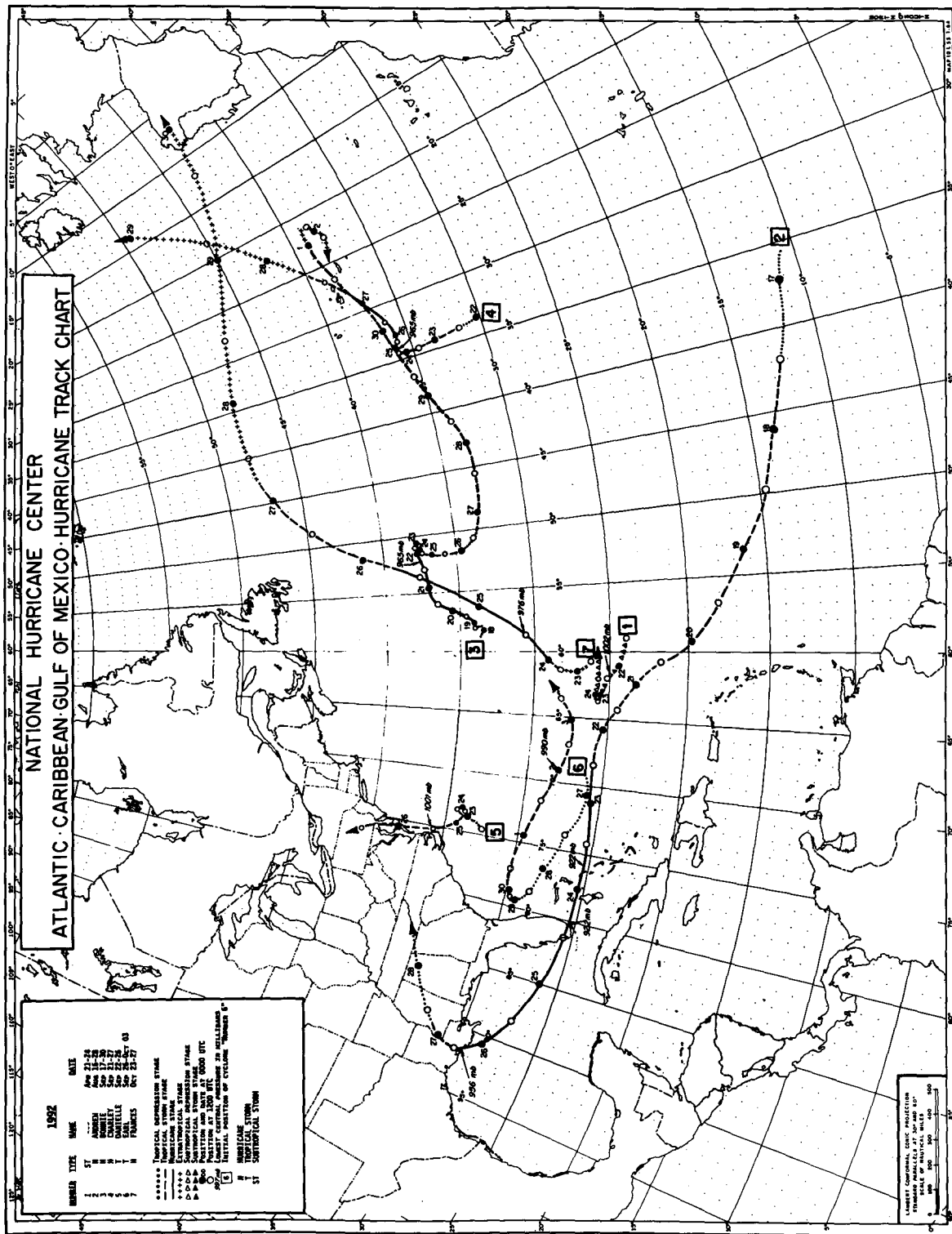
FIG. 1. Best tracks of the 1992 Atlantic subtropical storm, tropical storms, and hurricanes.

TABLE 1. 1992 Atlantic hurricane season statistics.

Number	Name	Class*	Dates**	Maximum l-min wind (m s⁻¹)	Minimum sea level pressure (mb)	U.S. damage ($ billions)	Direct deaths
1	One	ST	21–24 April	23	1002		
2	Andrew	H	16–28 August	69	922	20–25	26
3	Bonnie	H	17–30 September	49	965		1
4	Charley	H	21–27 September	49	965		
5	Danielle	T	22–26 September	28	1001		1
6	Earl	T	26 September–3 October	28	990		
7	Frances	H	23–27 October	39	976		

* T—tropical storm, wind speed 17–32 m s⁻¹ (34–63 kt). H— hurricane, wind speed 33 m s⁻¹ (64 kt) or higher. ST—subtropical storm, wind speed 17–32 m s⁻¹ (34–63 kt).

** Dates begin at 0000 UTC and include tropical depression stage.

Figure 2 also represents the changing environment through which Andrew moved. Note the zone of stronger than normal shear extending from 20°N, 70°W northeastward through the Atlantic. The tropical cyclone became extremely weak when it crossed over that area. As it approached the Bahamas, it moved into a region of anomalously weak shear and intensified into a severe hurricane.

2. Individual storms

a. Subtropical Storm One, 21–24 April

A nonfrontal low- to midtropospheric low pressure system became cutoff in the southwestern North Atlantic Ocean, centered near 25°N, 60°W, on 21 April. This is about 1100 km southeast of Bermuda. On this date, satellite imagery showed a large comma-shaped cloud pattern associated with the low. Ship reports indicated that the low was also present at the surface, and the subtropical depression stage is designated at 1200 UTC 21 April.

The subtropical depression moved toward the northwest initially near 5 m s⁻¹ but its motion gradually slowed over the next two days. A report from a ship with call sign C6KD7 indicated that the depression strengthened to a subtropical storm at 0600 UTC 22 April. The ship was located at 25.0°N, 61.0°W and reported a wind speed of 23 m s⁻¹ and a pressure of 1004.1 mb. Its pressure tendency indicated that the pressure had been even lower during the preceding 3 h. This is the basis for estimating the maximum wind speed of 23 m s⁻¹ and minimum surface pressure of 1002 mb 22 April. By 1800 UTC on the next day, the storm was downgraded to a tropical depression after an Air Force Reserve unit reconnaissance plane reached the system and reported that the minimum pressure had risen to 1008 mb and there were no longer any (sub)tropical storm–force winds in association with the center. A 1°C temperature rise in the cyclone center at a flight level of 500 m was also reported, suggesting the possibility that this was a borderline warm-core system. This, along with the presence of some convection near the center, comes close to satisfying the criteria for the definition of a tropical cyclone. The system became nearly stationary on 23 April as strong upper-level westerly winds began to affect the area.

A motion toward the east began early on 24 June and the system deteriorated to a low-level cloud swirl that dissipated during the next 24 h.
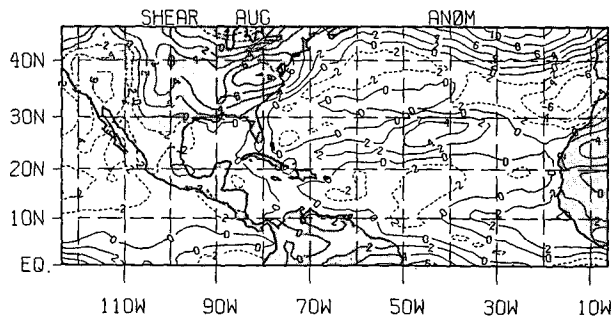

FIG. 2. Anomalies (from the 1975–1992 average) of the magnitude of vertical wind shear (upper- minus lower-tropospheric winds) for August of 1992. Units are meters per second.
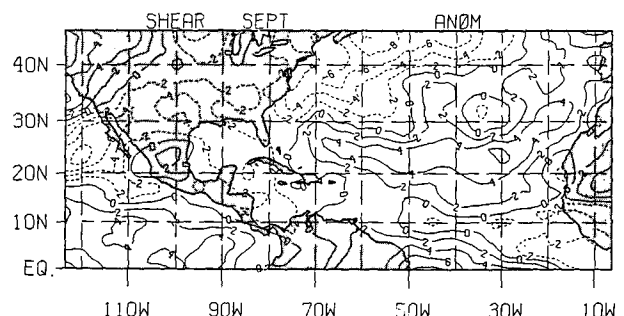

FIG. 3. Anomalies (from the 1975–1992 average) of the magnitude of vertical wind shear (upper- minus lower-tropospheric winds) for September of 1992. Units are meters per second.

b. Hurricane Andrew, 16–28 August

1) SYNOPTIC HISTORY

Satellite pictures and upper-air data indicate that Hurricane Andrew formed from a tropical wave that crossed from the west coast of Africa to the tropical North Atlantic Ocean on 14 August 1992. The wave moved westward at about 10 m s^{-1}, steered by a swift and deep easterly current on the south side of an area of high pressure. The wave passed to the south of the Cape Verde Islands on the following day. At that point, meteorologists at the NHC Tropical Satellite Analysis and Forecast (TSAF) unit and the Synoptic Analysis Branch (SAB) of the National Environmental Satellite Data and Information Service (NESDIS) found the wave sufficiently well organized to begin classifying the intensity of the system using the Dvorak (1984) analysis technique.

Convection subsequently became more focused in a region of cyclonic cloud rotation. Narrow spiral-shaped bands of clouds developed around the center of rotation 16 August. At 1800 UTC 16 August, both the TSAF unit and SAB calculated a Dvorak T number of 2.0, and the transition from tropical wave to tropical depression took place at that time.

The depression was initially embedded in an environment of easterly vertical wind shear. By midday on 16 August, however, the shear diminished. The depression grew stronger and at 1200 UTC 17 August it became Andrew, the first Atlantic tropical storm of the 1992 hurricane season. The tropical cyclone continued moving rapidly on a heading that turned from west to west-northwest. This course was in the general direction of the Lesser Antilles.

Between 17 and 20 August, the tropical storm passed south of the center of the high pressure area over the
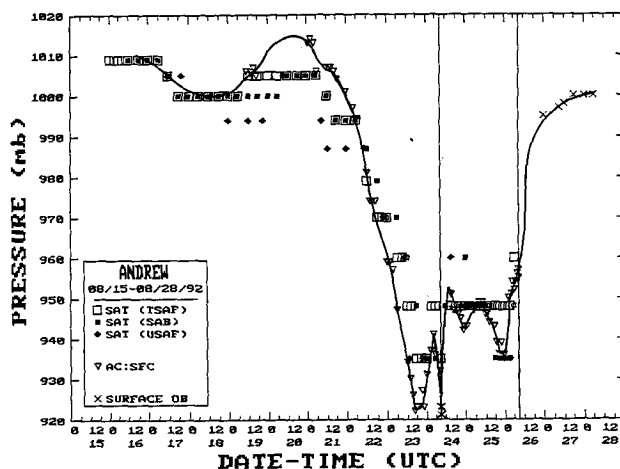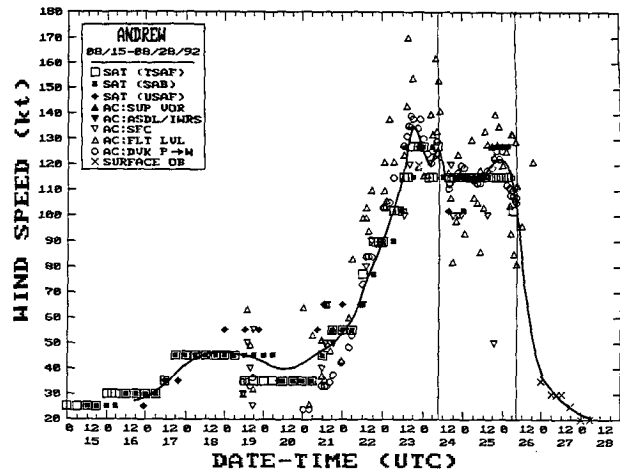

FIG. 5. Best-track maximum sustained wind speed curve for Hurricane Andrew, August 1992 (1 kt = 0.51 m s^{-1}). Not all aircraft observations are a sampling of the maximum wind. Landfalls on mainland noted by vertical lines.

eastern Atlantic. Steering currents carried Andrew closer to a strong upper-level low pressure system centered about 900 km to the east-southeast of Bermuda and to a trough that extended southward from the low for several hundred kilometers. These currents gradually changed and Andrew decelerated on a course that became northwesterly. This change in heading spared the Lesser Antilles from an encounter with Andrew. The change in track also brought the tropical storm into an environment of strong southwesterly vertical wind shear and quite high surface pressures to its north. Although the estimated maximum wind speed of Andrew varied little then, a rather remarkable evolution occurred.

Satellite images suggest that Andrew produced deep convection only sporadically for several days, mainly in several bursts of about 12-h duration. Also, the deep convection did not persist. Instead, it was stripped away from the low-level circulation by the strong southwesterly flow at upper levels. Air Force Reserve unit reconnaissance aircraft investigated Andrew and on 20 August found that the cyclone had degenerated to the extent that only a diffuse low-level circulation center remained. Andrew's central pressure rose considerably (Fig. 4). Nevertheless, the flight-level data indicated that Andrew retained a vigorous circulation aloft. Wind speeds near 36 m s^{-1} were measured at an altitude of 500 m near a convective band lying to the northeast of the low-level center. Hence, Andrew is estimated on 20 August to have been a tropical storm with 21 m s^{-1} surface winds and an astonishingly high central pressure of 1015 mb (Figs. 4 and 5).

Significant changes in the large-scale environment near and downstream from Andrew began by 21 August. Satellite imagery in a water vapor channel indi-

FIG. 4. Best-track central pressure curve for Hurricane Andrew, August 1992. Landfalls on mainland noted by vertical lines.

cated that the low aloft to the east-southeast of Bermuda weakened and split. The bulk of the low opened into a trough that retreated northward. That evolution decreased the vertical wind shear over Andrew. The remainder of the low dropped southward to a position just southwest of Andrew where its circulation enhanced the upper-level outflow over the tropical storm. At the same time, a strong and deep high pressure cell formed near the United States southeast coast. A ridge built eastward from the high into the southwestern North Atlantic with its axis lying just north of Andrew. The associated steering flow over the tropical storm became easterly. Andrew turned toward the west, accelerated to near 8 m s^{-1}, and quickly intensified.

Andrew reached hurricane strength on the morning of 22 August, thereby becoming the first Atlantic hurricane to form from a tropical wave in nearly two years. An eye formed that morning and the rate of strengthening increased. Just 36 h later, Andrew reached the borderline between a category 4 and 5 hurricane and was at its peak intensity. From 0000 UTC 21 August (when Andrew had a barely perceptible low-level center) to 1800 UTC 23 August the central pressure had fallen by 92 mb, down to 922 mb. A fall of 72 mb occurred during the last 36 h of that period and qualifies as rapid deepening (Holliday and Thompson 1979).

The region of high pressure held steady and drove Andrew nearly due west for two and a half days beginning on 22 August. Andrew was a category 4 hurricane when its eye passed over northern Eleuthera Island in the Bahamas late on 23 August and then over the southern Berry Islands in the Bahamas early on 24 August. After leaving the Bahamas, Andrew continued moving westward toward southeast Florida.

Andrew weakened when it passed over the western portion of the Great Bahama Bank, and the central pressure rose to 941 mb. However, the hurricane rapidly reintensified during the last few hours preceding landfall on Florida as it moved over the warm Straits of Florida. During that period, radar, aircraft, and satellite data showed a decreasing eye diameter and strengthening eyewall convection. Aircraft and inland surface data (Fig. 6) suggest that the deepening trend continued up to and slightly inland of the coast. For example, the eye temperature measured by the reconnaissance aircraft was at least 1°-2°C warmer at 1010 UTC (an hour after the eye made landfall) than it was in the last "fix" about 25–30 km offshore at 0804 UTC. These measurements suggest that the convection in the eyewall and the associated vertical circulation in the eye and eyewall became more vigorous as the storm moved onshore. The radar data indicated that the convection in the northern eyewall became enhanced with some strong convective elements rotating around the eyewall counterclockwise as the storm made landfall. Numerical models suggest that some enhancement of convection can occur at landfall due to increased
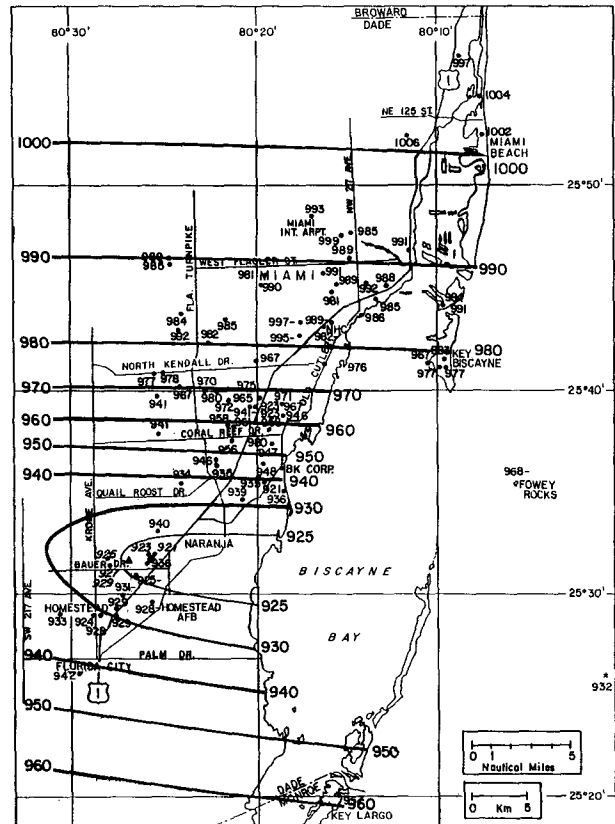

FIG. 6. Observations and smoothed analysis of minimum pressure during Hurricane Andrew's landfall in Florida. Minus sign indicates that a lower pressure may have occurred. The five italicized labels (near Bauer Dr.) show readings recalibrated and considered reliable in pressure chamber tests. Nearby bigger dot indicates neighborhood of lowest analyzed pressure (922 mb). Offshore reading of 932 mb reported from reconnaissance aircraft on plane's final pass through Andrew before landfall over Florida.

boundary-layer convergence in the eyewall region (e.g., Tuleya and Kurihara 1978; Tuleya et al. 1984; Jones 1987). That situation appeared to have occurred in Andrew. The enhanced convection in the north eyewall probably resulted in strong subsidence in the eye on the inside edge of the north eyewall. This likely contributed to a displacement of the lowest surface pressure to the north of the geometric center of the "radar eye" (cf. Figs. 6 and 7) by approximately 5 km in the vicinity of Homestead Air Force Base, Florida. It is estimated that the central pressure was 922 mb at landfall near Homestead at 0905 UTC 24 August (Fig. 6). An infrared satellite image of Andrew over southern Dade County is displayed in Fig. 8.

The maximum sustained surface wind speed (1-min average at 10-m elevation) during landfall over Florida is estimated at 64 m s^{-1}, with gusts at that elevation to at least 77 m s^{-1}. The sustained wind speed corresponds to a category 4 hurricane on the Saffir–Simpson hur-
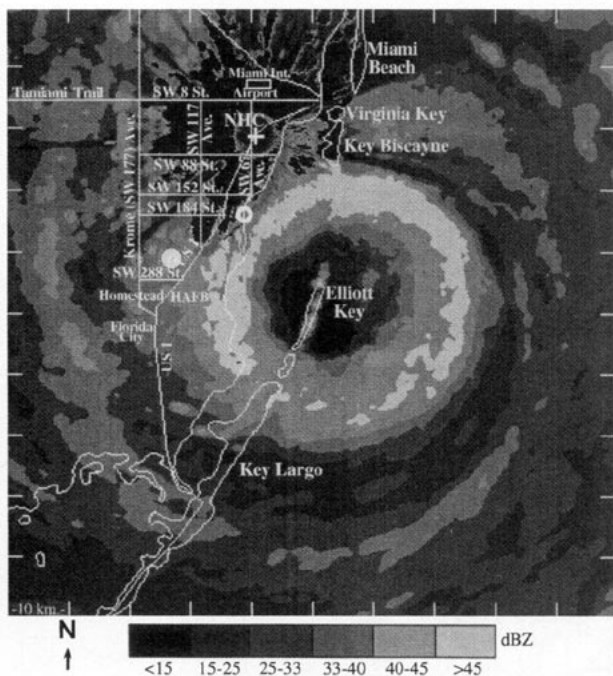
FIG. 7. Low-level radar reflectivity pattern (dBZ) obtained at 0835 UTC from last full sweep of the National Weather Service's Miami WSR-57 radar (located at the "+" identifying the National Hurricane Center) before Hurricane Andrew demolished part of equipment. Open white circle near coast indicates site of peak storm tide shown in Fig. 10. Solid white circle a little north of SW 288 St. shows neighborhood of lowest observed surface pressure (see Fig. 6). Radar data recorded and processed by the NOAA Hurricane Research Division.

ricane scale. It should be noted that these wind speeds are what is estimated to have occurred within the (primarily northern) eyewall in an open environment such as at an airport, at the standard 10-m height. The wind experienced at other inland sites was subject to complex interactions of the airflow with trees, buildings, and other obstacles in its path. These obstructions create a turbulent, frictional drag that generally reduces the wind speed. However, they can also produce brief, local accelerations of the wind immediately adjacent to the structures. Hence, the wind speed experienced at a given location, such as at a house in the core region of the hurricane, can vary significantly around the structure and cannot be specified with certainty. The landfall intensity is discussed further in subsection 2.

Andrew moved nearly due west when over land and crossed the extreme southern portion of the Florida peninsula in about 4 h. Although the hurricane weakened about one category on the Saffir–Simpson hurricane scale during the transit over land, and the pressure rose to about 950 mb, Andrew was still a major hurricane when its eyewall passed over the extreme southwestern Florida coast.

The first of two cycles of modest intensification commenced when the eye reached the Gulf of Mexico.

Also, the hurricane continued to move at a relatively fast pace while its track gradually turned toward the west-northwest.

As Andrew reached the north-central Gulf of Mexico, the high pressure system to its northeast weakened and a strong midlatitude trough approached the area from the northwest. Steering currents began to change. Andrew turned toward the northwest and its forward speed decreased to about 4 m s^{-1}. The hurricane struck a sparsely populated section of the south-central Louisiana coast with category 3 intensity at about 0830 UTC 26 August. The landfall location is about 35 km west-southwest of Morgan City, Louisiana.

Andrew weakened rapidly after landfall, to tropical storm strength in about 10 h and to depression status 12 h later. During this weakening phase, the cyclone moved northward and then accelerated northeastward. Andrew and its remnants continued to produce heavy rain that locally exceeded 250 mm near its track (see Table 2b). By midday on 28 August, Andrew had begun to merge with a frontal system over the mid-Atlantic states.

2) METEOROLOGICAL STATISTICS

The best track intensities were obtained from the data presented in Figs. 4–6 and Fig. 9. The first two of these figures show the curves of Andrew's central pressure and maximum sustained 1-min wind speed, respectively, versus time, along with the observations on which they were based. The figures contain relevant surface observations and intensity estimates derived from analyses of satellite images performed by the TSAF unit, SAB, and the Air Force Global Weather Central (USAF in figures). The aircraft data came from reconnaissance flights by the U.S. Air Force Reserve unit based at Keesler Air Force Base, Mississippi. Additional data were collected onboard a National Oceanic and Atmospheric Administration (NOAA) aircraft.

Table 2 lists a selection of surface observations. The anemometer at Harbour Island, near the northern end of Eleuthera Island in the Bahamas, measured a wind speed of 62 m s^{-1} for an unknown period shortly after 2100 UTC 23 August. That wind speed was the maximum that could be registered by the instrument. A higher speed may have occurred at a later time.

Neither of the two conventional measures of hurricane intensity, central barometric pressure, and maximum sustained wind speed were observed at official surface weather stations in close proximity to Andrew at landfall in Florida. Homestead Air Force Base and Tamiami Airport discontinued routine meteorological observations prior to receiving direct hits from the hurricane. Miami International Airport was the next closest station but it was outside of the eyewall by about 10 km when Andrew's center passed to its south.
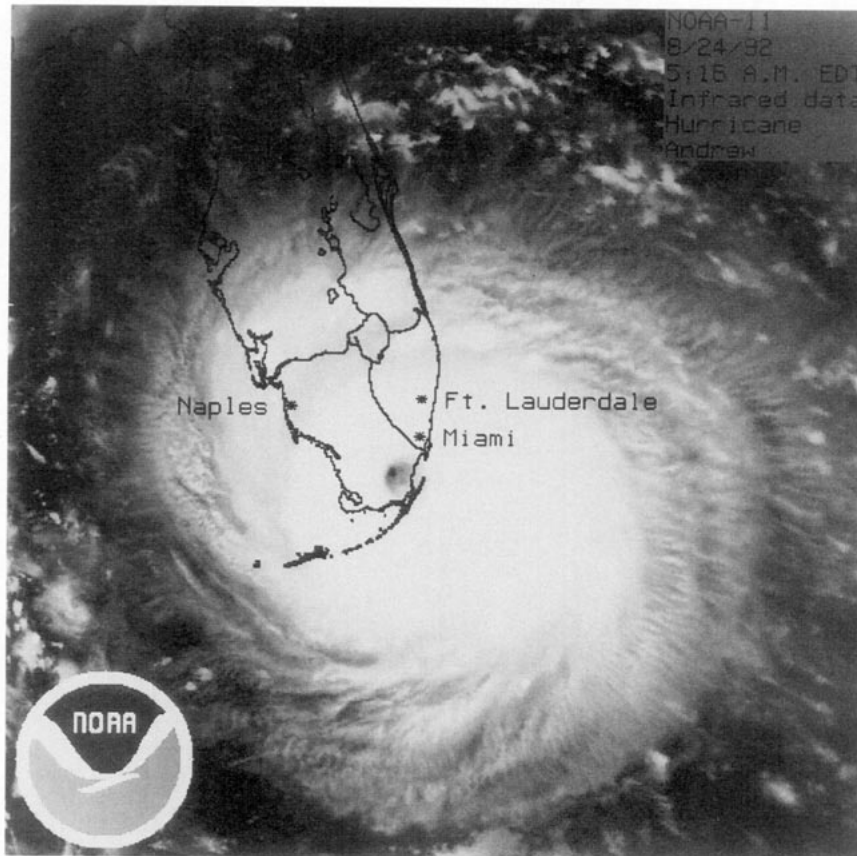
FIG. 8. *NOAA-11* infrared satellite image of Hurricane Andrew
taken a few minutes after the satellite's 0916 UTC equatorial crossing.

To supplement the official information, requests for data were made to the public through the local media. Remarkably, more than 100 quantitative observations have been received so far (see Figs. 6 and 7). Many of the reports came from observers who vigilantly took readings through frightening conditions, including—in several instances—the moments when their instruments and even their homes were destroyed.

Some of the unofficial observations were dismissed as unrealistic. Others were rendered suspect or eliminated during follow-up inquiries or analyses. The remainder, however, revealed a physically consistent and reasonable pattern.

(i) Minimum pressure over Florida

The final offshore "fix" by the reconnaissance aircraft came at 0804 UTC and placed the center of the hurricane only 25–30 km, or roughly 1 h of travel time, from the mainland. A dropsonde indicated a pressure of 932 mb at that time. The pressure had been falling at the rate of about 2 mb h^{-1} but the increasing interaction with land was expected to at least partially offset,

if not reverse, that trend. Hence, a landfall pressure within a few millibars of 932 mb seemed reasonable.

Shortly after Andrew's passage, however, reports of minimum pressures below 930 mb were received from the vicinity of Homestead (Fig. 6). Several of the barometers displaying the lowest pressures were subsequently tested in a pressure chamber and calibrated by the Aircraft Operations Center (AOC) of NOAA. The lowest accepted pressure in the AOC tests is 922 mb. Based on the observations and an eastward extrapolation of the pressure pattern to the coastline, Andrew's minimum pressure at landfall is estimated to be 922 mb. This suggests that the trajectory of the dropsonde deployed from the aircraft did not intersect the lowest pressure within the eye.

In any case, in the United States, this century, only the Labor Day (Keys') storm in 1935 (892 mb) and Hurricane Camille in 1969 (909 mb) had lower landfall central pressures than Andrew (Hebert et al. 1993).

(ii) Maximum wind speed over Florida

The strongest winds associated with Andrew on 24 August likely occurred in the hurricane's northern

TABLE 2a. Hurricane Andrew selected surface observations. Nonstandard wind speed averaging periods and anemometer heights are indicated where known.

Location	Minimum sea level pressure		Maximum surface wind speed (m s⁻¹)			Storm surge[b] (m)	Storm tide[b] (m)	Rain (storm total) (mm)
	Pressure (mb)	Date/time (UTC)	1-min average	Peak gust	Date/time[a] (UTC)			
Bahamas								
Harbour Island	935.0[c]	23/2100		62[c,d]	23/shortly after 2100			
Nassau	999.0[c]	24/0000	41	52	25/0025			
The Current						7.0		
Lower Bogue (1.8-km inland)						4.9		
Florida east coast and Keys								
Tamiami (TMB)	988.0[c,d]		57[c,d,e]		24/0848[f]			
Miami WSFO/NHC	982.0[c,d]	24/0900	52[c,d,g]	73[c,d,g]	24/0850			
NOAA/AOML	984.0			45[c,d]				
Miami International Airport (MIA)	992.6	24/0900	39[f]	52[f]	24/0950			51.8
Miami Beach			34[c]	47[c]	24/0816			
Haulover Pier	1004.0		30[c]	59	24/0900			
Fort Lauderdale (FLL)				27[c]				
Palm Beach (PBI)	1010.8	24/0259, 0420	22	26	24/1033			
Palm Beach ASOS			22		24/1036			
Key West WSO (EYW)	1010.1	24/1400	13	19	24/1614			8.4
Patrick Air Force Base (COF)	1016.2	24/0955	11	16	24/0735			
Melbourne (MLB)	1016.3	24/0950	8	11	24/1151			
Orlando (MCO)	1016.9	24/0950		15	24/1850			
NASA Shuttle (X68)	1016.9	24/0855	6	12	24/1755			
Titusville (TIX)	1017.9	24/1053	4	7	24/1149			20.3[c]
East Perrine							5.2 (see Fig. 6)	
Florida west coast								
Collier County EOC				45[g]				
Captiva Fire Station				32				
Fort Myers (RSW)	1010.2	24/1347, 1446	15	23	24/1446, 1547			14.2
Cape Coral								
Glades County EOC				23	24/between 1100 and 1200			
St. Petersburg/Clearwater Executive Airport			15	21	24/1625			
Goodland							1.8[h]	
Everglades City							1.8[h]	
Fort Myers Beach							0.6	
Venice							0.6	
Anna Marie Island							0.5	
Homosassa							0.5	
Gulf Harbors							0.5	
Indian Rocks Beach							0.3	
Louisiana								
Morgan City (P42)			41[g]	48[g]				
Baton Rouge (BTR)	996.5	26/1427	22	31	26/1452			144.8
New Orleans (MSY)	1006.6	26/0805	20	29	26/0950			144.8
Bayou Bienvenue								159.5
Salt Point AMOS (P92)			21	37	26/0728			
Lafayette (LFT)	990.5	26/1250	24	32	26/1057			139.6
Lake Charles (LCH)	1008.8		11	18	26/2152			1.3
Berwick Fire Station			43[g]	54[g]				
Jeanerette	975.0		37	40[c]				
Jeanerette			35	39	26/0845			
Near Brusly	990.2	26/1337	36	46[c]	26/1310			128.3
Lafayette Courthouse				46[g]				
Mooring 17 (29.2°N, 92.0°W)	994.9	26/0930						
Cocodrie							2.4	
Burns Point (St. Mary Parish)							2.1[i]	

TABLE 2a. (*Continued*)

Location	Minimum sea level pressure		Maximum surface wind speed (m s⁻¹)			Storm surge[b] (m)	Storm tide[b] (m)	Rain (storm total) (mm)
	Pressure (mb)	Date/time (UTC)	1-min average	Peak gust	Date/time[a] (UTC)			
Bayou Dupre							2.0	
Bayou Bienvenue							1.9	
NWS HANDAR east								
New Orleans							1.7	
Port Fourchon							1.5[i]	
North end of causeway							1.5	
Industrial canal							1.3	
Marina							1.3	
Rigolets							1.3	
Grand Isle							1.1[i]	
Alabama								
Huntsville (HSV)	1000.3	27/2250	11	19	27/1742			23.4
Birmingham (BHM)	1001.7	27/2215	10	18	27/1640			45.0
Montgomery (MGM)	1008.8	27/2045	12	16	27/2307			39.4
Mobile (MOB)	1010.1	27/2051	13	18	25/1844			16.3
Mobile State Docks						0.8	1.1	
Dauphin Island							1.8	
Georgia								
Atlanta (ATL)	1005.4	28/0400		20	27/2039			
Mississippi								
Jackson (JAN)	998.6	26/0750	14	25	27/0219			121.7
Tupelo (TUP)			12	19	27/2000			47.2
Meridian (MEI)	1004.4		13	25	27/0945			134.4
State Port (Gulfport)				39	27/1951			
Bay St. Louis							1.4[f]	
Texas								
Port Arthur (BPT)	1011.5	26/1000	11	15	26/1953			
Sabine Pass						0.3	0.4	
Ship reports								
OYGK2 (29.5°N, 80.6°W)			31		25/1200			
ELLE2 (19.4°N, 56.6°W)	1013.5	19/1500	18		19/1500			
C6KD (28.1°N, 79.2°W)	1015.5	24/0600	18		24/0600			
Gulf of Mexico platforms[c,g]								
SS 198G (28.2°N, 92.0°W)			40	52	26/0330			
EC 83H (28.2°N, 92.0°W)			24	25	26/0330			
EC 42B (29.5°N, 92.8°W)			20	45	26/0430			
SM 136B (28.2°N, 92.0°W)			20	23	25/2230			

[a] Time of 1-min wind speed unless only gust is given.

[b] *Storm surge* is water height above normal tide level. *Storm tide* is water height relative to National Geodetic Vertical Datum, which is defined as mean sea level in 1929.

[c] A more extreme value may have occurred.

[d] Equipment became inoperable after this measurement.

[e] Subsequent laboratory tests at the NHC indicate that the needles on the two wind speed dials at Tamiami Airport "peg" at about 53.8 and 55.6 m s⁻¹, respectively.

[f] Estimated.

[g] Nonstandard elevation.

[h] Above mean low water.

[i] Above mean water level.

Table 2b. Selected rainfall totals associated with Hurricane Andrew, August 1992. The asterisk indicates estimate.

Location	Total rain (mm)	Location	Total rain (mm)
Florida		Kentucky	
S-124 (Broward County)	197.9	BLWK2	65.0
S-21A (Dade County)	188.2		
S-20G (Dade County)	131.8	Mississippi	
S-37A (Broward County)	130.6	Sumrall	236.2
S-39 (Broward and Palm Beach counties)	130.0	Pelahatchie (gauge)	208.3
S-80 (Martin–St. Lucie)	125.5	Yazoo City	193.8
Everglades Park (Collier County)	*114.3	Crystal Springs	183.9
S-18C (Dade County)	113.8	Pelahatchie (co-op)	179.6
S-20F (Dade County)	104.6	Collins	178.8
Marco Island	*88.9	Union Church	178.8
S-308 (Lake Okeechobee area)	88.1	Brookhaven	178.3
Cudjoe Key	51.3	Mize	170.4
		Rockport	161.5
Louisiana		Monticello	161.5
Hammond	302.8	Booneville	160.0
Robert	279.9	Good Hope	156.0
Amite	263.1	Vicksburg	151.1
Morgan City	236.5	McComb	150.6
Manchee	225.3	Ofahoma	147.8
Jeanerette	202.2	Bay St. Louis	145.3
Butte La Rose	200.7	White Oak	143.5
Ponchatoula	191.5	Forest	142.0
Mt. Herman	190.5	Liberty	142.0
Franklin	178.6	Goshen Springs	140.2
WSFO Slidell	128.5	Port Gibson	140.0
Jena 4WSW	112.3	Meadville	138.4
		Tylertown	136.7
Alabama		Columbia	135.1
Aliceville	111.8	Philadelphia	128.5
Tuscaloosa	91.4		
MRGA1 Morgan	87.9	North Carolina	
MRZA1 Mount Roszell	81.5	HDSN7 Highlands	118.9
CDCA1 Red Bay Creek	73.7	WLGN7 F-Wallace Gap	69.3
WRTA1 Wright	73.4	RMNN7 Rosman	66.5
CBTA1 Colbert	69.8		
AKDA1 Lexington	67.6	Tennessee	
OAKA1 Oakland	66.5	ELKT1 Elkton	96.5
		WNBT1 Waynesboro	92.5
Georgia		GEOT1 Georgetown	87.1
Hurst	133.1	IRCT1 Iron City-Shoal Creek	84.6
Mountain City	116.8	BGLT1 Big Lick	82.5
Burton	109.5	CBOT1 Crab Orchard	78.0
Clayton	109.2	CLLT1 Collinwood	78.0
Nacoochee Georgia Power	97.3	PSKT1 Pulaski	77.0
Helen	86.4	LNVT1 Lynnville	75.4
SCHG1 Suches Grizzly Creek	84.3	PICT1 Pickwick Dam	74.9
TUSG1 Titus	79.5	CLET1 Cleveland	73.9
Tallulah	77.5	CLBT1 Columbia	71.1
Jasper	67.8	DYNT1 Dime	69.6
BRDG1 Blue Ridge Dam	67.3	LEWT1 Lewisburg	65.5
EPWG1 Epworth Higdon's Store	67.1	CSV Crossville Memorial Airport	65.3
		PKVT1 Pikeville	63.5

eyewall. The relatively limited number of observations in that area greatly complicates the task of establishing Andrew's maximum sustained wind speed and peak gust at landfall in Florida. While a universally accepted value for Andrew's wind speed at landfall may prove elusive, there is considerable evidence supporting an estimate of about 64 m s^{-1} for

the maximum sustained wind speed, with gusts to at least 77 m s^{-1} (Fig. 9).

The strongest reported sustained wind near the surface occurred at the Fowey Rocks weather station at 0800 UTC (Fig. 9). The station sits about 20 km east of the shoreline and, at that time, was within the northwest part of Andrew's eyewall. The 0800

TABLE 2c. Hurricane Andrew selected National Data Buoy Center observations, August 1992.

Platform/location	Minimum sea level pressure		Maximum wind speed[a] (m s^{-1})		
	Pressure (mb)	Date/time (UTC)	Average	Peak gust	Date/time (UTC)
Fowey Rocks C-MAN FWYF1/25.6°N, 80.1°W	967.5[b,c]	25/0800	63[b,c]	76[b,c]	24/0800
Bullwinkle Platform BUSL1/27.9°N, 90.9°W	998.5	25/2300	27	32[b]	25/2225
Molasses Reef C-MAN MLFR1/25.0°N, 80.4°W	998.5	24/0900	25	30	24/1000
Eastern Gulf Buoy 42003/25.9°N, 85.9°W	997.4	25/0400	23	32	25/0250
Grand Isle C-MAN GDIL1/29.2°N, 90.0°W	1005.2	25/2300	25	38	25/2200
Southwest Pass C-MAN BURL1/28.9°N, 89.4°W	1006.1	25/2200	29	41	25/2100
Sombrero Key C-MAN SMKF1/24.6°N, 81.2°W	1007.7	24/1100	18	22	24/1130
Lena Platform C-MAN LNEL1/28.2°N, 89.1°W	1007.7	25/1600			
Eleuthera Buoy 41016/24.6°N, 76.5°W	1007.9	23/2040	15	18[b]	24/0040
Sand Key C-MAN SANF1/24.5°N, 81.9°W	1010.2	24/1100, 1400	15	22	24/1600
Central Gulf Buoy 42001/25.9°N, 89.7°W	1010.8	25/0950	12	15	25/1650
Settlement Point C-MAN SPGF1/26.7°N, 79.0°W	1012.7	24/0600	20	24	24/0500
Buoy 42007/30.1°N, 88.8°W	1013.5	25/2250	15	24	25/1850
Dauphin Island C-MAN DPIA1/30.2°N, 88.1°W	1016.1	26/0000	17	24	25/2100

[a] NOAA buoys report hourly an 8-min average wind. C-MAN station reports are 2-min average winds at the top of the hour and 10-min averages at the other times. Contact NDBC for additional details.

[b] A more extreme value may have occurred.

[c] Equipment became inoperable shortly after observation.

UTC data included a 2-min wind of 63 m s^{-1} with a gust to 76 m s^{-1} at a platform height of about 40 m. The U.S. National Data Buoy Center (NDBC) used a boundary-layer model to convert the sustained wind to a 2-min wind of 56 m s^{-1} at 10 m elevation. The peak 1-min wind during that 2-min period at Fowey Rocks might have been slightly higher than 56 m s^{-1}.

It is unlikely that this point observation was so fortuitously situated that it represents a sampling of the strongest wind. The Fowey Rocks log (not shown) indicates that the wind speed increased through 0800 UTC. Unfortunately, Fowey Rocks then ceased transmitting data, presumably because even stronger winds disabled the instrumentation. (A subsequent visual inspection indicated that the mast supporting the anemometer had become bent 90° from vertical.) Radar reflectivity data suggests that the most intense portion of Andrew's eyewall had not reached Fowey Rocks by 0800 UTC and that the wind speed could have continued to increase there for another 15–30 min. A similar con-

clusion can be reached from the pressure analysis in Fig. 6, which indicates that the pressure at Fowey Rocks probably fell by about another 20 mb from the 0800 UTC mark of 968 mb.

Reconnaissance aircraft provided wind data at a flight level of about 3000 m. The maximum wind speed along 10 s of flight track (often used by the NHC to represent a 1-min wind speed at flight level) on the last pass prior to landfall was 83 m s^{-1}, with an instantaneous wind speed of 87 m s^{-1} observed. The 83 m s^{-1} wind occurred at 0810 UTC in the eyewall region about 19 km to the north of the center of the eye. Like the observation from Fowey Rocks, the aircraft provided a series of point observations (i.e., no lateral extent). Almost assuredly, somewhat higher wind speeds occurred elsewhere in the northern eyewall, a little to the left and/or to the right of the flight track. A wind speed at 3000 m is usually reduced to obtain a surface wind estimate. Based on past operational procedures, the 83 m s^{-1} flight-level wind is compatible with maximum sustained surface winds of 64 m s^{-1}.
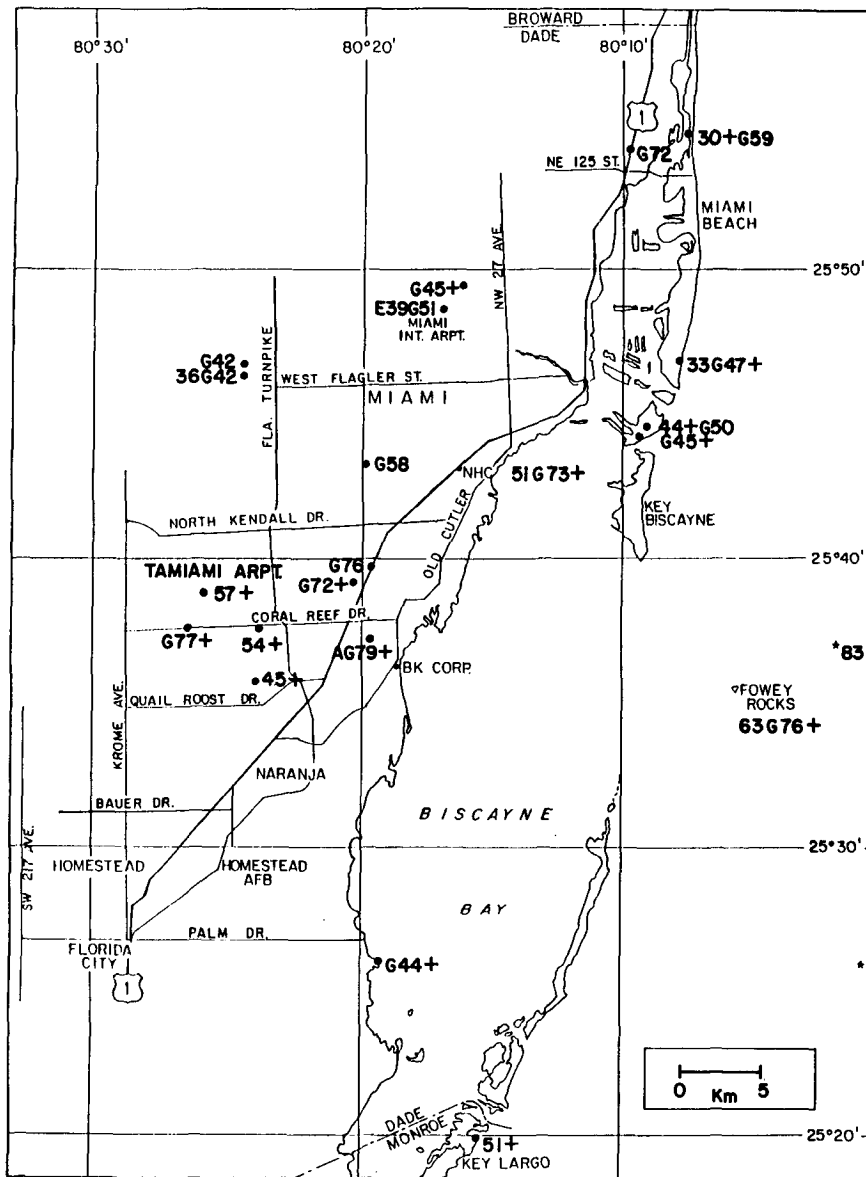
FIG. 9. Sustained wind speeds and gusts "G" in meters per second observed over southeast Florida in association with Hurricane Andrew. Offshore reading of 83 m s^{-1} occurred on board reconnaissance aircraft. The "+" follows observation(s) taken where higher speeds may have occurred. The "E" indicates estimate; "A" indicates reading adjusted to 79 m s^{-1} (from 95 m s^{-1} reported by observer).

One of the most important wind speed reports came from Tamiami Airport, located about 17 km west of the shoreline. As mentioned earlier, routine weather observations ended at the airport before the full force of Andrew's (northern) eyewall winds arrived. However, the official weather observer there, S. Morrison, remained on station and continued to watch the wind speed dial. Morrison notes that at approximately 0848 UTC the wind speed indicator "pegged" at a position a little beyond the dial's highest marking of 51 m s^{-1}, at a point that he estimates

corresponds to about 57 m s^{-1}. He recounts that the needle was essentially fixed at that spot for 3–5 min and then fell back to 0 when the anemometer failed. Morrison's observations have been closely corroborated by two other people. He has also noted that the weather conditions deteriorated even further after that time and were at their worst no sooner than 15 min later. This information suggests that, in all likelihood, the maximum sustained wind speed at Tamiami Airport significantly exceeded 57 m s^{-1}.

A number of the wind speeds reported by the public could not be substantiated and are therefore excluded from Fig. 9. The reliability of some of the others suffer from problems that include nonstandard averaging periods and instrument exposures, and equipment failures prior to the arrival of the strongest winds.

The only measurement of a sustained wind in the southern eyewall came from an anemometer on the mast of an anchored sailboat (see Fig. 9). For at least 13 min the anemometer there showed 51 m s^{-1}, which was the maximum that the readout could display. A small downward adjustment of the speed should probably be applied because the instrument was sitting 17 m above the surface rather than at the standard height of 10 m. On the other hand, the highest 1-min wind speed during that 13-min period could have been quite a bit stronger than 51 m s^{-1}. Again, there may have been stronger winds elsewhere in the southern eyewall. Bear in mind that (to a first approximation for a westward-moving hurricane) the wind speed in the northern eyewall usually exceeds the wind speed in the southern eyewall by about twice the forward speed of the hurricane (Dunn and Miller 1964). In the case of Andrew, that difference is about 16 m s^{-1}, and suggests a maximum sustained wind stronger than 67 m s^{-1} in the northern eyewall.

Several indirect measures of the sustained wind speed are of interest. First, a standard empirical relationship between central pressure and wind speed (Kraft 1961) applied to 922 mb yields around 69 m s^{-1}. Second, the Dvorak technique classification performed by the NHC TSAF unit using a 0900 UTC satellite image gives 65 m s^{-1}. Also, an analysis of the pressure pattern in Fig. 6 gives a maximum gradient wind of around 72 m s^{-1}.

The strongest, credible wind gust reported from near the surface occurred in the northern eyewall about 2 km from the shoreline at the home of R. Fairbank. He observed a gust of 95 m s^{-1} on a digital readout a few moments before a portion of a wall of his home collapsed, which prevented further observation. The hurricane also destroyed the anemometer. An inspection was made of the anemometer height and exposure, which verified that the instrument was at the 10-m level and it had an open exposure to the east, which was the direction of the wind at the time of failure. To evaluate the accuracy of the instrument, three anemometers of the type used by Fairbank were tested in a wind tunnel at Virginia Polytechnic Institute and State University. Although the turbulent nature of the hurricane winds could not be replicated, the results of the wind tunnel tests suggest that the actual wind at the time Fairbank read 95 m s^{-1} on his digital readout was 79 m s^{-1}. Of course, stronger gusts may have occurred there at a later time.

Strong winds also occurred outside of the eyewall, especially in association with convective bands (Fig. 7). A peak gust to 72 m s^{-1} was observed at a home

near the northern end of Dade County (Fig. 9) on an anemometer of the brand used by Fairbank. Applying the reduction suggested by the wind tunnel tests to 72 m s^{-1} yields an estimate of 60 m s^{-1}. This is nearly identical to the 59 m s^{-1} peak gust (a 5-s average) registered on a National Ocean Survey anemometer located not far to the east, at the coast.

(iii) Storm surge

Andrew came onshore in the northwest Bahamas and southeast Florida near high tide (+0.6–0.8 m) and was accompanied by a locally huge storm surge. The surge at The Current (a settlement near the northern end of Eleuthera Island) reached a phenomenal 7 m. Figure 10 shows the height of the storm tide (which is the sum of the storm surge and astronomical tide) over the southeast Florida coastline. The 5.2-m storm tide that headed inland from Biscayne Bay is a record maximum for the southeast Florida peninsula. The maximum storm tide on the Florida southwest coast is estimated at 1.5–2.1 m. Storm tides in Louisiana were at least 2.4 m (Table 2a) and caused flooding from Lake Borgne westward through Vermillion Bay.

(iv) Tornadoes

There have been no confirmed reports of tornadoes associated with Andrew over the Bahamas or Florida. However, funnel sightings, some unconfirmed, were reported in the Florida counties of Glades, Collier, and Highlands, where Andrew crossed in daylight. In Louisiana, one tornado occurred in the city of Laplace several hours prior to Andrew's landfall. That tornado killed 2 people and injured 32 others. Tornadoes in the Ascension, Iberville, Baton Rouge, Pointe Coupee, and Avoyelles parishes of Louisiana reportedly did not result in casualties. Numerous reports of funnel clouds were received by officials in Mississippi, and tornadoes were suspected to have caused damage in several Mississippi counties. In Alabama, the occurrence of two damaging tornadoes has been confirmed over the mainland, while another tornado may have hit Dauphin Island. As Andrew and its remnants moved northeastward over the eastern states, it continued to produce severe weather. For example, several damaging tornadoes in Georgia late on 27 August were attributed to Andrew.

(v) Rainfall

Andrew dropped sufficient rain to cause local floods even though the hurricane was relatively small and generally moved rather fast. Rainfall totals in excess of 175 mm were recorded in southeast Florida, Louisiana, and Mississippi (Table 2b). Rainfall amounts near 125 mm occurred in several neighboring states.
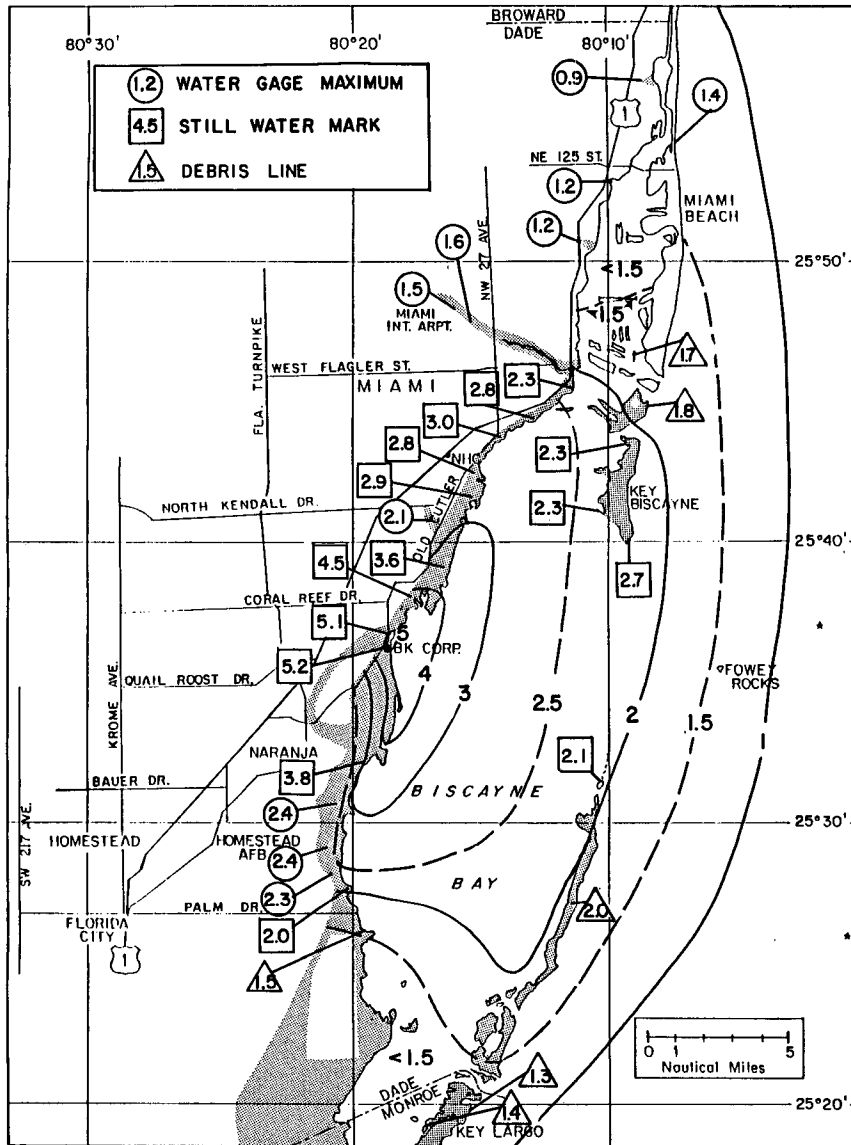
FIG. 10. Analysis and representative observations of the maximum storm tide during Hurricane Andrew's landfall in Florida, labeled in meters above 1929 mean sea level. Shading indicates inland inundation.

Hammond, Louisiana reported the highest total, near 303 mm.

3) CASUALTY AND DAMAGE STATISTICS

Table 3 lists a count of casualties and damages associated with Andrew. The number of deaths directly attributed to Andrew is 26. The additional indirect loss of life brought the death toll to 62 as of 7 September 1992. A combination of good hurricane preparedness and evacuation programs likely helped minimize the loss of life. Nevertheless, the fact that *no* lives were lost in the United States due to storm surge is viewed as a fortunate aberration.

Unfortunately, the count of indirect deaths has increased since 7 September. *The Miami Herald* reported on 31 January 1993 that it could relate at least 43 additional (indirect) deaths in Dade County to Hurricane Andrew.

Damage is estimated at $20–$25 billion. Andrew's impact on southern Dade County was extreme from the Kendall district southward through Homestead and Florida City to near Key Largo. Andrew reportedly destroyed 25 524 homes and damaged 101 241 others.

TABLE 3. Deaths and damages incurred in association with Hurricane Andrew. Based, in part, on reports from the Dade County Medical Examiner and Louisiana Office of Public Health for their respective jurisdictions. Note: *The Miami Herald* reported on 31 January 1993 that it could relate at least 43 additional (indirect) deaths in Dade County to Hurricane Andrew.

| | Deaths | | Damage ($ billion) |
	Direct	Indirect	
Bahamas	3	1	0.25
Florida	15	28	20–25
Dade County	15	24	20–25
Broward County	0	3	0.1
Monroe County	0	1	0.131
Collier County	0	0	0.03
Louisiana	8	7	1
St. John the Baptist Parish	2		
Offshore	6		
Lafayette Parish			
Vermillion Parish		1	
Iberville Parish		1	
Terrebonne Parish		3	
Orleans Parish		1	
Plaquemines Parish		1	
Georgia			0.001
Total	26	36	20–25

The Dade County Grand Jury reported that 90% of all mobile homes in south Dade County were totally destroyed. In Homestead, more than 99% (1167 of 1176) of all mobile homes were completely destroyed. *The Miami Herald* reported $0.5 billion in losses to boats in southeast Florida. The damage to Louisiana is estimated at $1 billion. Damage in the Bahamas has been estimated at $0.25 billion.

Andrew whipped up powerful seas that extensively damaged many offshore structures, including the artificial reef system of southeast Florida. For example, the Belzona Barge is a 66-m, 300 000-kg barge that, prior to Andrew, was sitting in 21 m of water on the ocean floor. About 900 000 kg of concrete from the old Card Sound bridge lay on the deck. The hurricane moved the barge about 200 m to the west (50 000–100 000 kg of concrete remain on deck) and removed several large sections of steel plate sidings.

Damage in the Gulf of Mexico is preliminarily estimated at $0.5 billion. *Ocean Oil* reported the following in the Gulf of Mexico: 13 toppled platforms, 5 leaning platforms, 21 toppled satellite structures, 23 leaning satellites, 104 incidents of structural damage, 7 incidents of pollution, 2 fires, and 5 drilling wells blown off location.

Figure 7 displays a radar reflectivity pattern about 30 min prior to landfall on southern Florida, superimposed on a map of that region. The figure shows that the average diameter of the eye was about 20 km

at landfall. The most devastated areas correspond closely in location to the region overspread by Andrew's eyewall and its accompanying core of destructive winds and, near the coastline, decimating storm surges. Flight-level data about an hour prior to landfall place the radius of maximum wind at 20 km (in the northern eyewall at 3000-m altitude). The radius of maximum wind at the surface was likely a little less than 20 km. Areas of southern Florida well outside the eyewall experienced less severe damage and fewer casualties. Table 3 reveals that more than one-half of the fatalities were indirect. Many of the indirect deaths occurred during the "recovery phase" following Andrew's passage.

Hurricanes are notoriously capricious. Andrew was a compact system. A little larger system, or one making landfall just a few kilometers farther to the north, would have been catastrophic for heavily populated, highly commercialized, and no less vulnerable areas to the north. That area includes downtown Miami, Miami Beach, Key Biscayne, and Fort Lauderdale. Andrew also left the highly vulnerable New Orleans region relatively unscathed.

4) WARNINGS

Table 4 lists the watch and warning lead times for landfall sites. (A complete chronology of watches and warnings issued by the NHC and the Government of the Bahamas is listed in the Diagnostic Report of the NHC available from the National Climatic Data Center, Federal Building, Asheville, North Carolina 28801.)

Massive evacuations were ordered in Florida and Louisiana as the likelihood of Andrew making landfall in those regions increased. About 55 000 people left the Florida Keys. Evacuations were ordered for 517 000 people in Dade County, 300 000 in Broward County, 315 000 in Palm Beach County, and 15 000 in St. Lucie County. For counties further west in Florida, evacuation totals exceeding 1000 people are Collier (25 000), Glades (4000), and Lee (2500). It is estimated that 1 250 000 people evacuated from parishes in southeastern and south-central Louisiana. About 250 000

TABLE 4. Watch and warning lead times for landfall sites during Hurricane Andrew. Lead time refers to time lapsed from advisory to landfall.

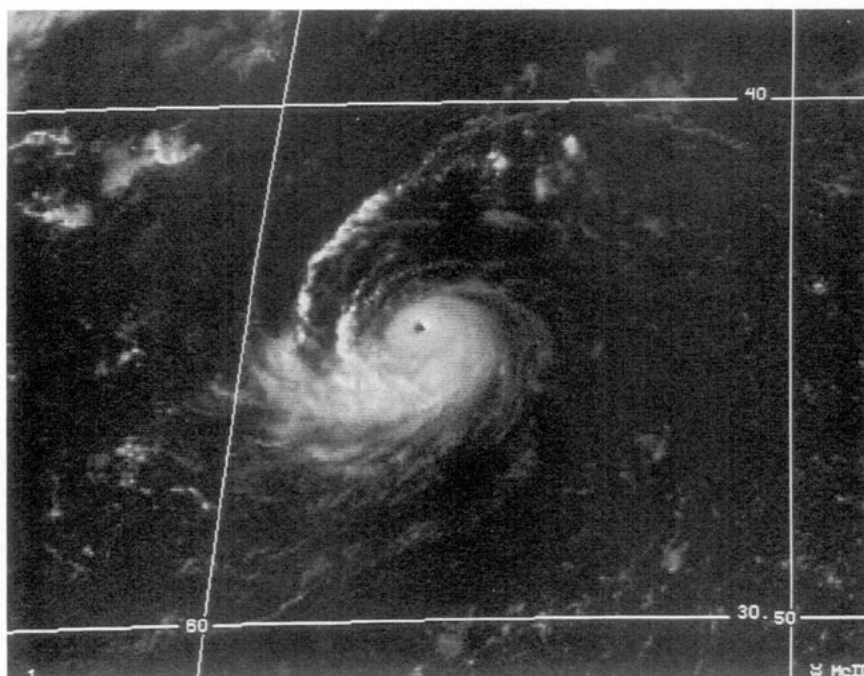| Location	Type	Lead time (h)
Northwest Bahamas	Hurricane watch	30
	Hurricane warning	24
Southeast Florida	Hurricane watch	36
	Hurricane warning	21
South-central Louisiana	Hurricane watch	43
	Hurricane warning	24

FIG. 11. *Meteosat-3* visible satellite image of Hurricane Bonnie at 1930 UTC 19 September 1992.

people evacuated from Orange and Jefferson counties in Texas.

The recovery process continues in several areas. Nevertheless, it is not too early to emphasize an important point. The winds in Hurricane Andrew wreaked tremendous structural damage, particularly in southern Dade County. Notwithstanding, the loss of life in Hurricane Andrew, while very unfortunate, was far less than has previously occurred in hurricanes of comparable strength. Historical data suggests that storm surge is the greatest threat to life. Some lives were likely saved by the evacuation along the coastline of southeast Florida. The relatively small loss of life there serves as testimony to the success and importance of coordinated programs of hurricane preparedness.

c. Hurricane Bonnie, 17–30 September

Bonnie had its origins in a nontropical weather system. A cold front moved off the east coast of the United States on 11 September. The front moved southeastward and then became stationary, with its western end in the vicinity of Bermuda by 15 September. Surface pressures fell over an area a few hundred kilometers east-northeast of Bermuda on the following day, and satellite pictures on 17 September showed that an area of cloudiness had become detached and isolated from the frontal cloud band. The cloud pattern quickly became organized, exhibiting cyclonically curved bands and a small circularly shaped overcast feature. The

tropical depression stage of Bonnie began at 1800 UTC 17 September.

The depression strengthened fairly rapidly and became Tropical Storm Bonnie around 0600 UTC 18 September. As is frequently the case in nontropical-type developments, Bonnie was initially embedded within a larger-scale deep-layer cyclonic circulation. This provided an environment of relatively weak vertical shear that also controlled the steering of Bonnie during the early stages. Bonnie moved slowly along a counterclockwise path before strengthening into a hurricane at 1800 UTC 18 September. The hurricane commenced an east-northeast to northeast motion on 19 September while exhibiting a fairly well-defined eye (Fig. 11). The eye became indistinct at times on 20 September, but satellite images showed that it had again become rather sharp in appearance on 21 September. At 1800 UTC 21 September, Bonnie reached its peak intensity with maximum winds of 49 m s^{-1} estimated from satellite imagery.

The forward speed, which was already slow, decreased even further on 22 September. Bonnie was practically stationary from 1800 UTC 22 September until 1200 UTC 23 September, when it began drifting west-southwestward. Bonnie then weakened considerably. Satellite imagery showed that the low-level center became exposed from the associated deep convection. Winds decreased to tropical storm strength on 24 September. By 25 September, Bonnie had lost most of its deep convection and by 0000 UTC 26 September

had weakened briefly to a tropical depression. However, tropical storm strength was regained a little later on that day as deep convection returned.

Bonnie began a southward motion on 24 September that continued until 26 September, when the storm turned southeastward and then eastward, while picking up some forward speed. The stalling and southward drift of Bonnie were related to the northward retreat of deep-layer westerlies over the west-central Atlantic and the formation of a blocking-type pattern in the steering currents. A midtropospheric high built to the northwest of Bonnie and forced the tropical cyclone southward. Subsequently, a broad deep-layer trough developed over the Atlantic to the east of Bonnie. The combined effects of the trough and high guided Bonnie southward for a while. Later on, as the influence of the trough became dominant, Bonnie was steered southeastward and eastward.

Although Bonnie had strengthened back to a tropical storm, it remained in a westerly shearing environment on 26 and 27 September. The circulation center was generally near the western edge of the deep convective overcast. However, on 27 September, Bonnie's cloud pattern took on a nontropical comma shape and the deep convection was confined to an area several degrees east of the center. By 28 September, convection had returned near the center and Bonnie looked more like a tropical storm again. The system was then moving toward the east-northeast and it maintained that course for the next couple of days with some increase in forward speed. The center of the storm, moving near 10 m s^{-1}, passed through the Azores island group on 30 September. Lajes Air Force Base in the Azores had showers and squalls as Bonnie approached. Observers at Lajes reported sustained winds of 18 m s^{-1} with gusts to 26 m s^{-1} as Bonnie passed. Wind gusts to 30 m s^{-1} were reported atop a 73-m tower on the island. Deep convection diminished and, shortly after passing through the Azores, Bonnie became an extratropical low. The low then decelerated and looped clockwise, eventually moving back toward the Azores while dissipating.

One death was reported as a result of a rockfall on the island of St. Michaels in the Azores related to Bonnie.

d. Hurricane Charley, 21–27 September

Meteosat imagery showed that cloudiness and showers became concentrated in an area centered about 1000 km south of the Azores early on 20 September. Animation of the satellite imagery suggested that a mid- to upper-level cyclonic circulation was interacting with the northern portion of a tropical wave. By midday on 20 September, an inverted trough was analyzed in this vicinity on the NHC surface analysis. Visible imagery showed a well-defined low-level circulation on 21 Sep-

tember, and satellite classifications were initiated on this day. The system became a tropical depression at 1800 UTC 21 September about 1000 km southwest of the Azores. The depression initially moved toward the northwest near 5 m s^{-1}.

Satellite imagery showed increased convective banding on 22 September, and the system became Tropical Storm Charley at 1200 UTC on this day. The storm moved generally toward the north for the next couple of days, steered in part by the flow around the slowly moving Hurricane Bonnie located about 1850 km to the northwest. An eye appeared in the satellite pictures of Charley, and the system became a hurricane at 1200 UTC 23 September. Analysis of satellite imagery suggests that the maximum sustained winds were 49 m s^{-1} and minimum central pressure was 965 mb near 1800 UTC 24 September. Figure 12 is a visible satellite image of Charley near its peak intensity.

Charley began drifting in a general eastward direction by 25 September in association with a slowly changing deep-layer mean flow. On 26 September, Charley began moving toward the east-northeast with increasing forward speed over progressively cooler water. Charley was downgraded to a tropical storm at 0000 UTC 27 September, while centered just southwest of the Azores. The storm then accelerated toward the northeast and the center passed over the island of Terceira near 1000 UTC 27 September. Lajes Air Force Base reported a minimum pressure of 982.4 mb, with a sustained wind of 24 m s^{-1} and gusts to 37 m s^{-1}.

The storm gradually lost its tropical characteristics as it moved over the cooler water, and it became an extratropical cyclone at 1800 UTC 27 September. The acceleration toward the northeast continued until the system was absorbed by a larger extratropical low centered to the northwest of the British Isles near 0600 UTC 29 September.

The NHC has not received reports of casualties or damage related to Charley.

e. Tropical Storm Danielle, 22–26 September

1) SYNOPTIC HISTORY

Danielle originated on 22 September within an area of low pressure first detected over the Atlantic near the southeast United States coast on 18 September. It is also speculated that a weak tropical wave, which passed from Africa into the Atlantic on 8 or 9 September, moved into the area of formation on 18 September. A cold front had merged with the northern portion of this stationary weather system on 20 September.

By 22 September, surface reports and satellite imagery showed that a cyclonic circulation became better defined in the area of formation about 325 km south-southeast of Cape Hatteras, North Carolina, and it is estimated that a tropical depression formed there near 1200 UTC on this day. An Air Force Reserve unit
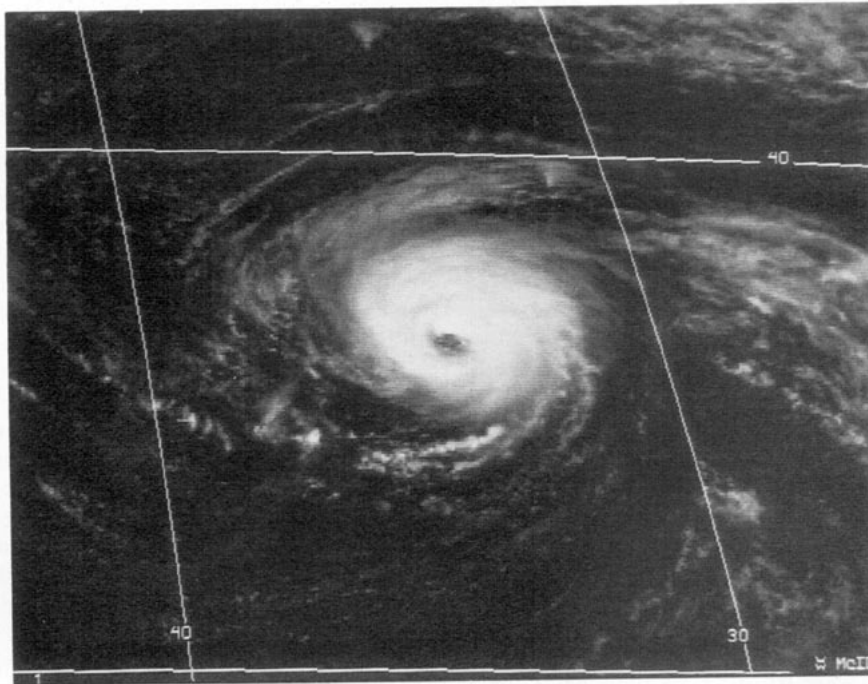
FIG. 12. *Meteosat-3* visible satellite image of Hurricane Charley
at 1430 UTC 24 September 1992, a few hours before its maximum strength.

aircraft reconnoitered the system several hours later and reported 23 m s^{-1} flight-level winds, and the depression was upgraded to Tropical Storm Danielle.

In response to an approaching trough in the westerlies, Danielle moved slowly northeastward, but the trough passed and was replaced by high pressure to the north of the storm. This resulted in Danielle executing a small clockwise loop on 23 and 24 September, followed by a westward motion toward the Outer Banks of North Carolina on 25 September. However, the storm soon turned northward when a large extratropical low approached the Great Lakes and, in combination with high pressure anchored to the east of the storm, set up a southerly steering current. Some strengthening occurred while the storm paralleled the coast of North Carolina. Sustained winds increased to 28 m s^{-1} and the central pressure fell to 1001 mb.

The center of the storm moved inland late on 25 September, over the Delmarva section of Maryland. The weakening storm moved across Maryland and Delaware and over eastern Pennsylvania on 26 September, where it dissipated.

2) METEOROLOGICAL STATISTICS

The maximum wind reported by aircraft was 32 m s^{-1} at an elevation of 500 m at 1704 UTC 25 September, while the minimum central pressure was 1001 mb several hours earlier. Peak satellite intensity estimates were 23 m s^{-1} and 1000 mb.

Table 5 is a listing of selected surface observations. There were several coastal reports of tropical storm–force winds. The highest sustained wind speed reported was 23 m s^{-1} at Cape Charles, Virginia. A few reports of 17 m s^{-1} wind speeds or higher were also received from observers on board ships. A report of 33 m s^{-1} from the ship *Stonewall Jackson* is suspected of being somewhat too high, although it was near the center of the storm at the time and its pressure of 1001 mb agrees with the aforementioned reconnaissance value. Also, data buoys as far north as New York Harbor reported tropical storm–force winds.

The storm was within range of several radars including Cape Hatteras; Patuxent River Naval Air Station, Maryland; the WSR-88D radar at Sterling, Virginia; and, for a short period, Atlantic City, New Jersey. These showed an increasingly better presentation of a center and heavier convection prior to landfall, which allows for the possibility that the 33 m s^{-1} ship report might not be too far off.

Storm rainfall totals were near 100 mm over central Virginia and up to 75 mm along the extreme eastern portions of Virginia, Maryland, Delaware, and New Jersey. Eastern Pennsylvania had up to 50 mm of rain. The highest storm surge reported was 1.6 m above normal astronomical tide at Cape Hatteras.

3) CASUALTY AND DAMAGE STATISTICS

One death occurred. It was the result of a sailboat being battered and sunk by high seas to the east of New

TABLE 5. Tropical Storm Danielle selected surface observations, September 1992.

Location	Minimum sea level pressure		Maximum surface wind speed (m s^{-1})			Storm surge (m)	Rain (storm total) (mm)
	Pressure (mb)	Date/time (UTC)	1-min average	Peak gust	Date/time (UTC)*		
North Carolina							
Alligator River Bridge			21	26	25/0000		
Cape Hatteras (HAT)	1006.9	25/0745	13	22	25/0226	1.6	5
Cedar Island Ferry			16	21	25/0500		
Diamond Shoals Light				24			
Manteo				24	25/1000		
Ocracoke Island	1010.4	25/1800	19	23	25/0300		
Virginia							
Cape Charles			23	25	25/1800		
Cape Henry				27	25/0900 (24 m above ground)		
Charlottesville							104
Norfolk	1015.6	25/1834	13	25	25/1151	0.7	9
Maryland							
Baltimore/Washington Airport (BWI)							67
Salisbury							71
Delaware							
Cape Henlopen				29	25/2300		
Indian River Inlet (USCG)			22	27			
Odessa							74
Smyrna							95
Wilmington							58
Washington National Airport (DCA)			10	13	26/0351		29

* Time of sustained wind speed unless only gust is given.

Jersey. There was minor flooding and significant beach erosion along the mid-Atlantic coast. According to press reports, only minor damage resulted from the storm.

4) WARNINGS

The storm made landfall at 2200 UTC 25 September on the Delmarva peninsula only 12 h after the tropical storm warning was issued for the landfall area and 25 h after the watch was issued. Warnings were extended northward from North Carolina through Rhode Island in four steps over a 24-h period as the storm turned and moved northward across the mid-Atlantic states.

f. Tropical Storm Earl, 26 September–3 October

A tropical wave exited the coast of Africa on 18 September and for several days moved westward through low latitudes accompanied by disorganized cloudiness and showers. Once the wave approached the Lesser Antilles, it began to interact with a large and strong upper-level trough that was partially related to the outflow from Danielle and Bonnie located at higher latitudes.

Due to the interaction with the upper trough, most of the convection associated with the wave shifted further to the north within a band along 62°W between 22° and 28°N. The upper trough developed into a cutoff low while moving southwestward toward central Cuba. This new pattern may have enhanced the upper-level difluence over the convection associated with the wave, perhaps contributing to the wave becoming a tropical depression about 650 km north of Hispaniola by 1800 UTC 26 September.

The weak depression moved rapidly on a west-northwest course toward the northern Bahamas, steered by the flow induced, in part, by the middle- to upper-level low over Cuba. However, a cold front sweeping across the eastern United States forced the depression to become nearly stationary over the warm waters of the Gulf Stream. There, the depression strengthened.

Data from an Air Force Reserve unit reconnaissance plane, buoys, and ships indicate that the depression became Tropical Storm Earl at 1200 UTC 29 September. By then Earl was already moving eastward ahead of the cold front. The tropical storm was able to maintain its low-level circulation, staying detached from the surface frontal boundary for several days. It reached its peak intensity of 28 m s^{-1} and 990 mb at 0000 UTC 2 October.
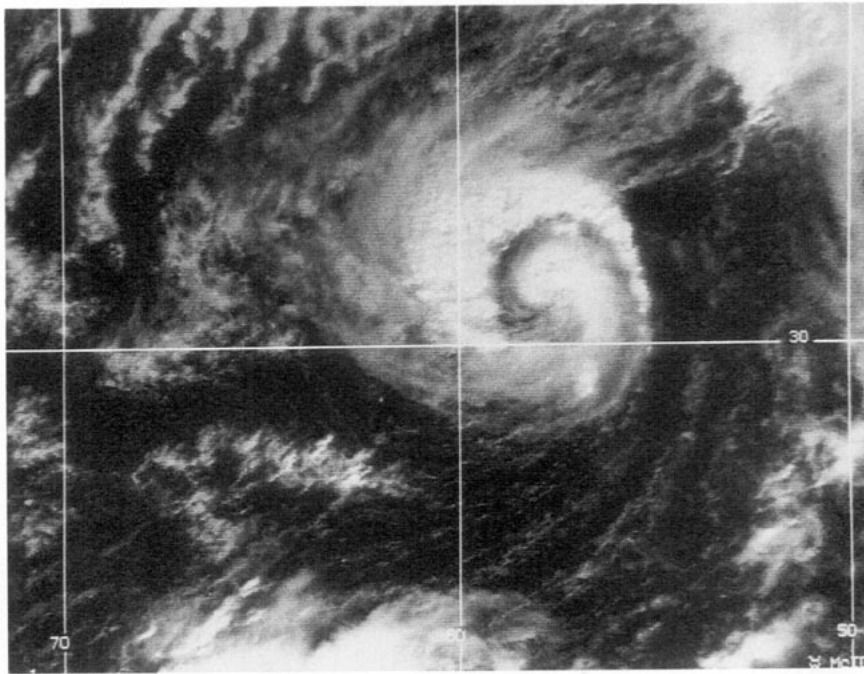
FIG. 13. *GOES-7* visible satellite image of Hurricane Frances
at 1400 UTC 24 October 1992, shortly after its maximum strength.

Earl continued moving on a general east-southeast track, producing transient convection but maintaining a well-defined low-level circulation. Finally, the storm weakened to a tropical depression at 1200 UTC 3 October and lost its tropical characteristics later on that day. The remnants of Earl meandered over the Atlantic for a few more days until dissipation.

A tropical storm watch was issued for Eleuthera and Abaco islands at 1500 UTC 27 September and was discontinued at 2100 UTC on the same day. This action was taken by the Government of the Bahamas as a precautionary measure for small vessels in those islands. The winds associated with the circulation of the tropical cyclone were not expected to reach sustained tropical storm force over the United States east coast. Consequently, tropical storm watches or warnings were not issued there. However, due to strong northeasterly winds produced by the pressure gradient between Earl and a strong high pressure system centered over the United States east coast, a coastal flood watch was issued from New Smyrna Beach to Fernandina Beach, Florida. A tropical storm watch was issued for Bermuda at 2100 UTC 30 September and was discontinued 24 h later.

There were no reports of casualties or damage associated with Earl.

g. Hurricane Frances, 23–27 October

Frances formed about 750 km to the south-southeast of Bermuda. Satellite pictures and surface analyses in-

dicate that the formation occurred within a broad area of low pressure that developed near the trailing end of a weak, quasi-stationary frontal trough. A south-southwesterly vertical wind shear, associated with a nearly stationary upper-level trough located over the East Coast and the southwestern Atlantic Ocean, kept the western portion of the low free of deep convection from 18 through 21 October. In contrast, the eastern portion of the low remained under a long, nearly 400-km-wide band of clouds that extended from north-northwest to south-southeast. Satellite pictures suggest that the section of the band extending south-southeast from the low was periodically invigorated for several days by the northern portion of tropical waves.

Water vapor imagery on 22 and 23 October showed an upper-level cyclonic circulation system "cutting off" to the southwest of the low, within the upper-level trough. The shear then decreased and, with the possible enhancing effects of a tropical wave, the low quickly strengthened and became a gale center of about 1004 mb by 1800 UTC on 22 October. The deep convection then began to wrap cyclonically around the circulation center and quickly grow in lateral extent. This indicates that the system was making a transition from a gale center to Tropical Storm Frances. The transformation was completed shortly after 0600 UTC 23 October.

Several ship reports from the *Migaea* and *Sparrow* document that the cyclone strengthened during the transition period. The *Migaea* observed a pressure of 1000 mb about 275 km from the circulation center at

TABLE 6. Comparison of 1992 Atlantic official track forecast errors (km) with 1982–91 10-yr average. A track forecast error is defined as the great-circle distance between a forecast position and a postanalysis best-track position for the same time. Cases include all subtropical storms, tropical storms, and hurricanes.

	Forecast period (h)					
	0	12	24	36	48	72
1992 average	19	76	157	250	337	500
(number of cases)	(159)	(151)	(146)	(137)	(124)	(100)
1982–91 average	31	100	192		381	572
1982–91 (average number of cases)	(139)	(135)	(117)		(86)	(63)
1992 departure from 1982–91 average	−41%	−24%	−18%		−12%	−13%
1992 range	0–83	11–204	17–507	44–709	52–820	20–1182

2230 UTC 22 October. By 0200 UTC 23 October it was closer to the center and observed 997 mb with sustained winds of 26 m s^{-1} and gusts to 38 m s^{-1}. The *Sparrow* reported sustained winds of 26 m s^{-1} near 0000 UTC. Before sunrise, sustained winds approached 33 m s^{-1} at the *Sparrow* but then dropped temporarily to 17 m s^{-1} while the wind direction switched from southeast to northwest. Those changes coincided with the sky partially clearing and the pressure reaching 996 mb after falling rapidly for several hours. These observations suggest that the first stages in the formation of an eye occurred early on 23 October.

Frances continued to strengthen through 23 October. The ship *TSL Bold*, located 55–85 km southeast of the center of Frances, reported a pressure of 994 mb at 1600 UTC and a southwest wind of 33 m s^{-1} 4 h later. An eye appeared for the first time on satellite images during that period. The initial reconnaissance mission in the cyclone found a 979-mb central pressure at 2238 UTC. From these data it is estimated that Frances reached hurricane strength near 1800 UTC.

Frances initially drifted northward, in the general direction of Bermuda. By late on 23 October, however, the trough to the west of Frances was reinforced by a new midlatitude short-wave trough approaching from the eastern United States. The associated steering flow accelerated Frances northeastward to about 10 m s^{-1} on 24 October. Frances reached its peak intensity, with estimated 39 m s^{-1} sustained winds and 976-mb central pressure, on that day. Figure 13 is a visible satellite image of Frances shortly after its maximum strength.

The track toward the northeast carried Frances over colder water. The eye became indistinct on 25 October, although relatively deep convection persisted near the circulation center through early on 27 October. Analyses of surface weather maps indicate a gradual broadening of the wind field during that period. Frances became extratropical at about 0600 UTC 27 October. Over the following three days, Frances moved generally to the east as a complex extratropical gale.

The only injury associated with Frances reported to the NHC occurred to A. Page on board the 10-m sail-

TABLE 7. Official maximum 1-min wind speed forecast errors (m s^{-1}) for subtropical storms, tropical storms, and hurricanes in the Atlantic basin, 1992. Error = forecast − observed.

	Forecast period (h)				
	12	24	36	48	72
1992 mean	0.0	+0.5	+0.7	+1.1	+2.0
1992 mean absolute	3.5	6.0	8.1	10.0	13.8
(number of cases)	(151)	(145)	(138)	(122)	(100)
Maximum error	+21	+26	+36	+36	+44
1982–91 Mean	−1.0	−1.4		−2.9	−3.3
1982–91 average number of cases	131	113		81	58
1982–91 mean absolute	4.1	5.9		8.2	10.0
1992 departure from 1982–91 mean absolute	−14%	+01%		+21%	+38%

boat *Sparrow*. She suffered a broken rib, and the boat was partially disabled during her encounter with the cyclone on 22 and 23 October. No other reports of damage or casualties related to Frances have been received by the NHC.

3. Verification

The NHC issues "official forecasts" of the center position and maximum 1-min wind speed for all subtropical and tropical cyclones in the North Atlantic Ocean, Caribbean Sea, and Gulf of Mexico. These forecasts are issued at 6-h intervals, for the periods of 12, 24, 36, 48, and 72 h. After the season, the forecasts are evaluated by comparison with the "best track" postanalysis of all available data. Table 6 lists the official track error averages for 1992. These errors range from 19 km at the 0-h forecast period (initial position error) to 500 km at 72 h. The average 1992 track errors are less than the previous 10-yr averages at all time periods.

The average 1992 official wind speed forecast errors are listed in Table 7. The forecasts had a positive bias (an overestimate) at all forecast periods, with mean absolute errors increasing with the length of the forecast period. The mean absolute errors for 1992 beyond 12 h are somewhat larger than the corresponding previous 10-yr averages.

REFERENCES

Dunn, G. E., and B. I. Miller, 1964: *Atlantic Hurricanes.* Louisiana State University Press, 326 pp.

Dvorak, V. F., 1984: Tropical cyclone intensity analysis using satellite data. NOAA Tech. Rep. NESDIS 11, National Oceanic and Atmospheric Administration, U.S. Department of Commerce, Washington, D.C., 47 pp.

Hebert, P. J., J. D. Jarrell, and M. Mayfield, 1993: The deadliest, costliest, and most intense hurricane of this century (and other frequently requested facts). NOAA Tech. Memo. NWS NHC-31, National Oceanic and Atmospheric Administration, U.S. Department of Commerce, Washington, D.C., 40 pp.

Holliday, C. R., and A. H. Thompson, 1979: Climatological characteristics of rapidly intensifying typhoons. *Mon. Wea. Rev.,* **107,** 1022–1034.

Jones, R. W., 1987: A simulation of hurricane landfall with a numerical model featuring latent heating by the resolvable scales. *Mon. Wea. Rev.,* **115,** 2279–2297.

Kraft, R. H., 1961: The hurricane's central pressure and highest wind. *Mar. Wea. Log.,* **5,** 157.

Neumann, C. J., B. R. Jarvinen, A. C. Pike, and J. D. Elms, 1990: Tropical cyclones of the North Atlantic Ocean, 1871–1986. *Historical Climatology Series* 6-2, National Climatic Data Center, 186 pp.

Pasch, R. J., and L. A. Avila, 1994: Atlantic tropical systems of 1992. *Mon. Wea. Rev.,* **122,** 539–548.

Simpson, R. H., 1974: The hurricane disaster potential scale. *Weatherwise,* **27,** 169–186.

Tuleya, R. E., and Y. Kurihara, 1978: A numerical simulation of the landfall of tropical cyclones. *J. Atmos. Sci.,* **35,** 242–257.

——, M. A. Bender, and Y. Kurihara, 1984: A simulation study of the landfall of tropical cyclones using a movable nested-mesh model. *Mon. Wea. Rev.,* **112,** 124–136.